Coalescence of planar GaAs nanowires into strain-free three-dimensional crystals on exact (001) silicon

Qiang Li, Huaxing Jiang and Kei May Lau [a)]

Department of Electronic and Computer Engineering, Hong Kong University of Science and Technology, Clear Water Bay, Kowloon, Hong Kong

[a)] Tel: (852)23587049, Fax: (852) 23581485, Email: eekmlau@ust.hk

Abstract

We report three dimensional (3D) disk-shaped GaAs crystals on V-groove patterned (001) Si substrates by metalorganic chemical vapor deposition. Planar GaAs nanowires with triangular cross-sections were grown inside Si V-grooves by nano-scale selective heteroepitaxy. These nanowires were then partially confined in micro-sized SiO_2 cavities and coalesced into uniform arrays of 3D crystals. Scanning electron microscope and atomic force microscopy inspection showed the absence of antiphase-domains and smooth top surface morphology. Superior structural and optical properties over GaAs thin films on planar Si were also demonstrated. More remarkably, by growing the 3D crystals on V-grooved Si, we were able to overcome the residual tensile stress induced by the thermal mismatch between GaAs and Si. Strain-free GaAs was uncovered in the crystals with a dimension of $3 \times 3\ \mu m^2$.

Key words:

A1. Defects

A1. Stresses

A3. Metalorganic chemical vapor deposition

A3. Selective epitaxy

B2. Semiconducting III-V materials

B2. Semiconducting gallium arsenide

1. Introduction

Direct epitaxial growth of III-V compound semiconductors on silicon is an enabling technology for monolithic electronic-photonic integration in state-of-the-art CMOS processes [1]-[3]. The fundamental roadblock has been a large mismatch in lattice constants and thermal expansion coefficients between III-V materials and Si substrates. For blanket heteroepitaxy of GaAs on Si, the 4.1% lattice mismatch gives rise to a high dislocation density on the order of 10^9-10^{10}/cm^2, while the 120% thermal mismatch causes residual stress and macroscopic cracks in films beyond a certain critical thickness. Antiphase-domains (APDs) associated with polar on nonpolar growth pose another challenge.

Substrate patterning has been used in heteroepitaxy as it brings benefits of epitaxial defect necking effect and allows for effective strain relaxation [4]-[10]. Recently, we demonstrated the growth of planar GaAs nanowire arrays on V-groove patterned exact-(001) Si substrates [11]. Initializing GaAs growth on the exposed (111) Si surfaces prevents generation of antiphase-domains. Further merging the nanowires into large-area thin films resulted in device-quality (001) GaAs-on-Si templates suitable for quantum dot laser applications [12]-[13]. However, the residual stress induced by the large thermal mismatch in GaAs/Si heteroepitaxy has not been fully addressed in previous studies. In this work, we combine selective-area heteroepitaxy processes at nano- and micro- scales and demonstrate three-dimensional (3D) strain-free GaAs crystals on (001) silicon. The crystalline quality and optical properties have been compared with GaAs thin films that were grown on planar Si and on V-grooved Si substrates. Effective stress relaxation was uncovered in the crystals with reduced dimension, along with good material properties.

2. Experimental methods

The GaAs/Si heteroepitaxy was carried out in an AIX-200/4 metalorganic chemical vapor deposition (MOCVD) system. Fig. 1(a) schematically illustrates the growth process to obtain micro-sized GaAs crystals. We started with on-axis (001) Si substrates patterned with 40 nm-wide SiO_2 stripes and 90 nm spacing. After a brief dip in 1% diluted hydrofluoric acid, the patterned Si sample was immersed in a 45% potassium hydroxide (KOH) solution heated at 70 °C to expose silicon {111} crystalline planes by anisotropic etching. Afterwards, selective MOCVD was performed to grow approximately 70 nm thick GaAs wires just filling up the V-shaped pockets.

Fig. 1(b) displays 70° tilted-view SEM image of the GaAs nanowires with triangular cross-sections and SiO_2 stripes in between. The wires are continuous along the trenches, with obvious shallow voids on the surface. Previous studies showed that these wires would evolve into rhombus-shaped nanowires with smooth {111} facets by extending the growth time [11]. The SiO_2 stripes between the dense GaAs nanowires in Fig. 1(b) was removed subsequently using buffered oxide etch (BOE). A 300 nm-thick blanket SiO_2 film was then deposited using plasma enhanced chemical vapor deposition (PECVD) and patterned into 5 μm × 5 μm and 3 μm × 3 μm cavities, with a pattern pitch of 10 μm and 6 μm, respectively. The top-view SEM image in Fig. 2 show the two types of micro-cavities. Inside the cavities, GaAs wires have been exposed. The shallow voids appearing in Fig. 1(b) are also visible. The square patterns were initially designed to be aligned to the same direction, yet a 45° mis-rotation occurred for the smaller ones during the optical lithography. As a result, we obtained squares with side lengths of 5 μm along the <110> direction in Fig. 2(a) and squares with side lengths of 3 μm along the <100> direction in Fig. 2(b). The uneven edges of the cavities were transferred from the rough photoresist edges during the BOE wet etching process. Using the micro-sized patterns shown in Fig. 2, selective heteroepitaxy of GaAs was performed at 600 °C with a growth rate of 25 nm/min. The exposed nanowires inside the cavities coalesced into 1 μm thick 3D disk-shape crystals.

3. Results and discussion

Fig. 3(a) and (b) display top-view SEM images of the 5 μm × 5 μm and 3 μm × 3 μm GaAs crystalline disks, respectively. In spite of a few GaAs particles sparsely deposited on the SiO_2 mask, the array of GaAs disks show clean and flat (001) top surface. The morphology of the multifaceted GaAs disks is somewhat similar to previous studies on selective area epitaxy on GaAs [14] and InP [15, 16] substrates. The sidewall facets were determined by measuring their inclinations with respect to the (001) top surface. According to the AFM line scans on a 5 μm × 5 μm crystal in Fig. 3(c), the sidewall angles were found to be 54° and 45° (along line-1 and line-2), which indicate the corresponding sidewalls are {111} and {110} planes, respectively. Fig. 3(d) sketches the four {111} side facets and four {110} corner facets of the GaAs crystals deposited in squares with side lengths along the <110> direction. Growing GaAs crystals in <100> direction orientated squares in Fig. 3(b) resulted in reduced relative area of the {111} facets with respect to that of the {110} facets. The corresponding crystallography is sketched in Fig. 3(e). It is also noted that the

symmetry of the obtained GaAs disks in Fig. 3(a) and (b) varies and irregularities appear occasionally. This is originated from the imperfect shape of the initial SiO_2 mask. Employing e-beam lithography and reactive ion etching for SiO_2 patterning should improve the smoothness of pattern edges and achieve more symmetric GaAs crystals.

The material structural and optical properties of the 3D crystals were further characterized using atomic force microscopy (AFM), x-ray diffraction (XRD) and room temperature micro-photoluminescence (μPL). Another two GaAs-on-Si templates, one with 1 μm GaAs thin film grown on V-grooved Si and the other with 1 μm GaAs thin film on planar (001) Si with 1° offcut, have been prepared for benchmarking. The offcut angle of the planar Si substrate was determined by x-ray diffraction. Fig. 4 shows the AFM images of the three samples across a scan area of 2 × 2 μm^2. Comparable root-mean-square roughness values of 1.1 nm, 1.2 nm and 0.9 nm have been achieved for the 3D crystal, GaAs-on-V-grooved-Si and GaAs-on-planar-Si, respectively.

Due to the polar nature of III-V materials versus the non-polar nature of Si, epitaxial growth of III-V materials on (001) Si substrates can result in a large density of antiphase boundaries (APBs). APBs are planar defects comprising atomic bonds formed between III−III or V−V atoms. They are generated when monoatomic steps are present at a (001) orientated substrate surface. Traditionally, APB-free III-V epi-layers on (001) Si are achieved by using offcut substrates with a surface orientation slightly tilted toward the [110] direction. Beginning with a Si substrate with a 4-6° offcut angle, single atomic steps tend to reorganize into energetically more stable double steps under high temperature annealing conditions. As a result, APB can be minimized in the subsequent III-V hetero-epitaxy. In this work, both SEM and AFM characterizations suggest all the three samples are free of antiphase boundaries. However, the APB elimination mechanisms differ from the conventional approach. For GaAs disks or thin films on V-grooved Si, material growth is initiated on {111} facets produced in the Si along a <110> direction. M. Paladugu et al. [17] have shown that the crystallographic alignment between the Si and III-V materials in the V-grooves can avoid the introduction of APBs. Unlike the single atom steps of (001) planes, a single step on the Si (111) surface has the height of one Si (111) double-layer (0.31 nm) [18, 19]. Such steps might not lead to the formation of APBs in the III−V materials. For the blanket hetero-epitaxy on planar (001) Si in Fig. 4(c), the substrate surface is likely single-layer stepped since the offcut angle of 1° is not sufficiently large. Our experiments showed that APBs still appeared at the early stage of the GaAs/Si hetero-epitaxy but decreased with buffer growth. With ~300 nm GaAs

overgrown layer on Si, APBs have completely vanished. As a matter of fact, in our study, nominal Si (001) substrates with offcut angle as small as 0.4° can be used to achieve APB-free GaAs. These results coincide with recent observations from a number of groups that single domain Ge and III-V layers can be deposited on standard nominal Si (001) substrates [20, 21, 22].

XRD omega-rocking curve is widely used for assessment of defect density in materials of comparable thicknesses. We used an Empyrean system with a line-collimated x-ray beam for XRD measurement. Fig. 5 compares XRD omega-rocking curves measured from the three samples near the GaAs (004) reflection. The FWHM of the ω-rocking curve can be correlated with the threading dislocation density D (cm^{-2}) through the Ayers' model [23]:

$$D = \frac{\beta^2}{4.36b^2}$$

where β is the FWHM in radians, b is the length of burgers vector of dislocation. For 60° dislocations in GaAs, $b = \sqrt{2}a/2$, where a = 5.65 Å is the lattice constant of GaAs. D provides an estimate of upper limit of dislocation density in the GaAs. The GaAs thin film on V-grooved Si exhibited a full-width-at-half-maximum (FWHM) of 310 arcsec and has the highest peak intensity. According to Ayers' model, the FWHM value translates into a dislocation density of 3.2×10^8 cm^{-2}, in good agreement with the estimated dislocation density (~$10^8/cm^2$) from plan-view TEM [24]. In contrast, the 1 μm GaAs thin film on planar Si exhibited a greatly broadened rocking curve with a three-fold reduction in peak intensity and an increased FWHM of 644 arcsec, suggesting a dislocation density above 10^9 cm^{-2}. XRD measurement of the 3D GaAs crystals revealed a FWHM of 317 arcsec comparable to the thin film on V-grooved Si. Noted that the decreased intensity stemmed from the reduced material volume detectable by the x-ray beam. In spite of superior crystalline quality over the planar offcut template, patterning the GaAs nanowires to grow thin films (Fig. 4(b)) or 3D crystals (Fig. 4(a)) with present thickness show minimum difference. A larger height over width ratio is necessary to let threading dislocations escape from the sidewalls by the so-called aspect ratio trapping (ART) mechanism [5, 9, 25, 26] and bring additional defect reduction benefits compared to the large-area thin film on V-grooved Si.

Finally, we have performed room temperate μPL measurement to probe the optical properties and stress relaxation of the GaAs/Si samples. A 514 nm line of an Ar+ laser was used as the excitation source and the spot diameter of the focused laser beam on the sample was about 4 μm using a 50× objective. A reference sample consisting of 1 μm un-doped GaAs grown on a semi-

insulating GaAs substrate was added in the comparison. Fig. 6 displays the comparison of the PL curves obtained from the GaAs crystals and thin films on Si against the homoepitaxial GaAs reference. The lowest PL intensity from the GaAs layer on planar Si correlates with its highest dislocation density, whereas the thin films and 3D crystals on V-grooved Si show only a slight PL degradation compared to the reference GaAs. In terms of peak wavelengths, both the GaAs thin films on V-groove patterned Si and planar Si show clear red-shift, due to a residual tensile stress induced by the thermal mismatch in the cooling down stage from the epitaxial growth temperature. However, such PL red-shift was greatly mitigated in the 5 μm 3D crystals, owing to the reduced crystal dimension. More strikingly, the PL peak wavelength of the 3 μm crystals coincided with that of the homoepitaxial GaAs reference, signifying strain-free micro-sized GaAs crystals were obtained.

4. Conclusions

In conclusion, we have combined selective area MOCVD heteroepitaxy at nano- and micro-scales to grow 3D GaAs crystals on exact oriented (001) Si substrates. The GaAs crystalline disks exhibit smooth top (001) surfaces, good material qualities and are free of antiphase domains. The residual stress stemming from the thermal mismatch between GaAs and Si is overcome with decreasing disk size. This work therefore marks a step forward towards monolithic integration of GaAs based optoelectronic devices on industrial standard silicon platform.

Acknowledgements

This work was supported in part by Grants (614312 and 16212115) from the Research Grants Council of Hong Kong. The authors would like to thank SUNY Poly for providing the initial nano-patterned Si substrates, Y. Han for the assistance in lithography, and the MCPF and NFF of HKUST for the technical support. Helpful discussions with C. Liu and B. Shi are also acknowledged.

References:

[1] H. Kataria, W. Metaferia, C. Junesand, C. Zhang, N. Julian, J. E. Bowers, J. E., & S. Lourdudoss, Simple epitaxial lateral overgrowth process as a strategy for photonic integration on silicon, IEEE Journal of Selected Topics in Quantum Electronics, *20*(4), 380-386.

[2] Z. Wang, B. Tian, M. Pantouvaki, W. Guo, P. Absil, J. V. Campenhout, C. Merckling, and D. V. Thourhout, Room-temperature InP distributed feedback laser array directly grown on silicon, Nat. Photonics 9, 837 (2015)

[3] T. E. Kazior, More than Moore: III-V devices and Si CMOS get it together, IEDM Tech. Dig., Dec. 2013, pp.699-702.

[4] T.A. Langdo, C. W. Leitz, M. T. Currie, E. A. Fitzgerald, A. Lochtefeld, and D. A. Antoniadis, High quality Ge on Si by epitaxial necking, Appl. Phys. Lett. 76, no. 25 (2000): 3700-3702.

[5] J. Z. Li, J. Bai, J.-S. Park, B. Adekore, K. Fox, M. Carroll, A. Lochtefeld, and Z. Shellenbarger, Defect reduction of GaAs epitaxy on Si (001) using selective aspect ratio trapping, Appl. Phys. Lett. 91, 021114 (2007).

[6] C. Merckling, N. Waldron, S. Jiang, W. Guo, N. Collaert, M. Caymax, E. Vancoille, K. Barla, A. Thean, M. Heyns, and W. Vandervorst, Heteroepitaxy of InP on Si(001) by selective-area metal organic vapor-phase epitaxy in sub-50 nm width trenches: The role of the nucleation layer and the recess engineering, J. Appl. Phys. 115, 023710 (2014).

[7] Q. Li, K.W. Ng, C.W. Tang, K.M. Lau, R. Hill, A. Vert, Defect reduction in epitaxial InP on nanostructured Si (001) substrates with position-controlled seed arrays, J. Cryst. Growth, 405, pp.81-86.

[8] B. Zhang, H. Liang, Y. Wang, Z. Feng, K. W. Ng, and K. M. Lau, High-performance III-nitride blue LEDs grown and fabricated on patterned Si substrates, J. Cryst. Growth 298 (2007): 725-730.

[9] C.V. Falub, H. von Hans, F. Isa, R. Bergamaschini, A. Marzegalli, D. Chrastina, G. Isella, E. Müller, P. Niedermann, and L. Miglio., Scaling hetero-epitaxy from layers to three-dimensional crystals. Science 335, no. 6074 (2012): 1330-1334.

[10] A.G. Taboada, T. Kreiliger, C.V. Falub, F. Isa, M. Salvalaglio, L. Wewior, D. Fuster, M. Richter, E. Uccelli, P. Niedermann, and A. Neels, Strain relaxation of GaAs/Ge crystals on patterned Si substrates, Appl. Phys. Lett., 104(2), p.022112.

[11] Q. Li, K. W. Ng, and K. M. Lau, Growing antiphase-domain-free GaAs thin films out of highly ordered planar nanowire arrays on exact (001) silicon, Appl. Phys. Lett. 106, 072105 (2015)

[12] Y. Wan, Q. Li, A. Y. Liu, A. C. Gossard, J. E. Bowers, E. L. Hu, and K. M. Lau, Optically pumped 1.3 μm room-temperature InAs quantum-dot micro-disk lasers directly grown on (001) silicon, Optics Lett. 41, no. 7 (2016): 1664-1667.

[13] Y. Wan, Q. Li, A. Y. Liu, Weng W. Chow, A. C. Gossard, J. E. Bowers, E. L. Hu, and K. M. Lau, Sub-wavelength InAs quantum dot micro-disk lasers epitaxially grown on exact Si (001) substrates, Appl. Phys. Lett., 108, 221101 (2016).

[14] D. W. Shaw, Selective epitaxial deposition of Gallium Arsenide in holes, J. Electrochem. Soc 113 (1966) 904-908.

[15] J. Yuan, H. Wang, P. J. van Veldhoven, and R. Nötzel, Impact of base size and shape on formation control of multifaceted InP nanopyramids by selective area metal organic vapor phase epitaxy, J. Appl. Phys. 106, 124304 (2009).

[16] W. Metaferia, A. Dev, H. Kataria, C. Junesand, Y.-T. Sun, S. Anand, J. Tommila, G. Pozina, L. Hultman, M. Guina, T. Niemib and S. Lourdudoss, High quality InP nanopyramidal frusta on Si, CrystEngComm 16, 4624 (2014)

[17] M. Paladugu, C. Merckling, R. Loo, O. Richard, H. Bender, J. Dekoster, W. Vandervorst, M. Caymax, and M. Heyns, Site selective integration of III-V materials on Si for nanoscale logic and photonic devices, Cryst. Growth Des. 12 (2012) 4696.

[18] P. Allongue; V. Costakieling; H. Gerischer, Etching of Silicon in NaOH solutions, J. Electrochem. Soc. 140 (1993)1009

[19] J.-L. Lin, D. Y. Petrovykh, J. Viernow, F. K. Men, D. J. Seo, and F. J. Himpsel, Formation of regular step arrays on Si (111) 7×7, J. Appl. Phys. 84 (1998) 255.

[20] Y. Bogumilowicz, J. M. Hartmann, R. Cipro, R. Alcotte, M. Martin, F. Bassani, J. Moeyaert, T. Baron, J. B. Pin, X. Bao, Z. Ye and E. Sanchez, Anti-phase boundaries–Free GaAs epilayers on "quasi-nominal" Ge-buffered silicon substrates, Appl. Phys. Lett. 107 (2015) 212105.

[21] R. Alcotte, M. Martin, J. Moeyaert, R. Cipro, S. David, F. Bassani, F. Ducroquet, Y. Bogumilowicz, E. Sanchez, Z. Ye, X. Y. Bao, J. B. Pin and T. Baron, Epitaxial growth of antiphase boundary free GaAs layer on 300 mm Si(001) substrate by metalorganic chemical vapour deposition with high mobility, APL Mater. 4 (2016) 046101.

[22] T. Orzali, A. Vert, T.-W. Kim, P.Y. Hung, J. L Herman, S. Vivekanand, G. Huang, M. Kelman, Z. Karim, R. J. W. Hill, S. S. P. Rao, Growth and characterization of an $In_{0.53}Ga_{0.47}As$-based Metal-Oxide-Semiconductor Capacitor (MOSCAP) structure on 300mm on-axis Si (001) wafers by MOCVD, J. Crys. Growth 427 (2015) 72.

[23] J. E. Ayers, The measurement of threading dislocation densities in semiconductor crystals by X-ray diffraction, J. Crys. Growth, 135 (1994) 71.

[24] Y. Wan, Q. Li, Y. Geng, B. Shi, K. M. Lau, InAs/GaAs quantum dots on GaAs-on-V-grooved-Si substrate with high optical quality in the 1.3 μm band, Appl. Phys. Lett., 107(8), 081106.

[25] A. G. Taboada, M. Meduňa, M. Salvalaglio, F. Isa1, T. Kreiliger, C. V. Falub, E. Barthazy Meier, E. Müller, L. Miglio, G. Isella and H. von Känel, GaAs/Ge crystals grown on Si substrates patterned down to the micron scale, J. Appl. Phys. 119 (2016) 055301.

[26] T. Orzali, A. Vert, B. O'Brien, J. L. Herman, S. Vivekanand, R. J. W. Hill, Z. Karim, and S. S. Papa Rao, GaAs on Si epitaxy by aspect ratio trapping: Analysis and reduction of defects propagating along the trench direction, J. Appl. Phys. 118 (2015) 105307.

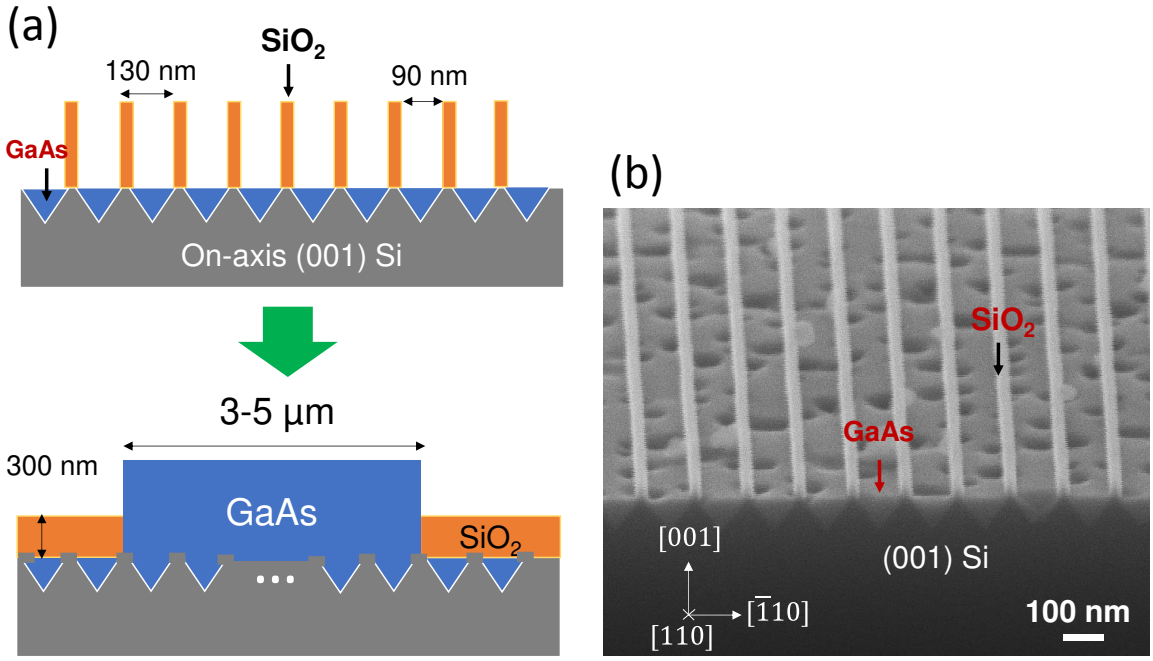

Figure 1. (a) Schematic of growing 3D GaAs crystals using patterned nanowires on V-grooved Si; (b) Tilted-view SEM image of GaAs wires grown inside Si V-grooves.

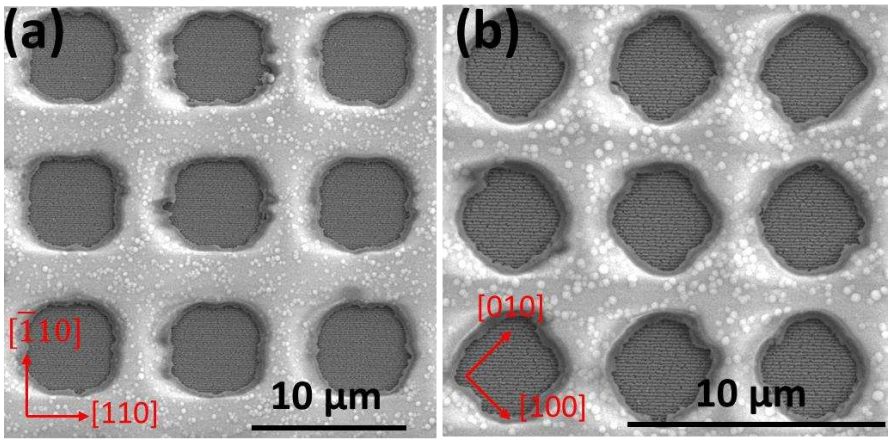

Figure 2. Top-view SEM image of SiO_2 square patterns with dimensions of 5 µm × 5 µm (a) and 3 µm × 3 µm (b).

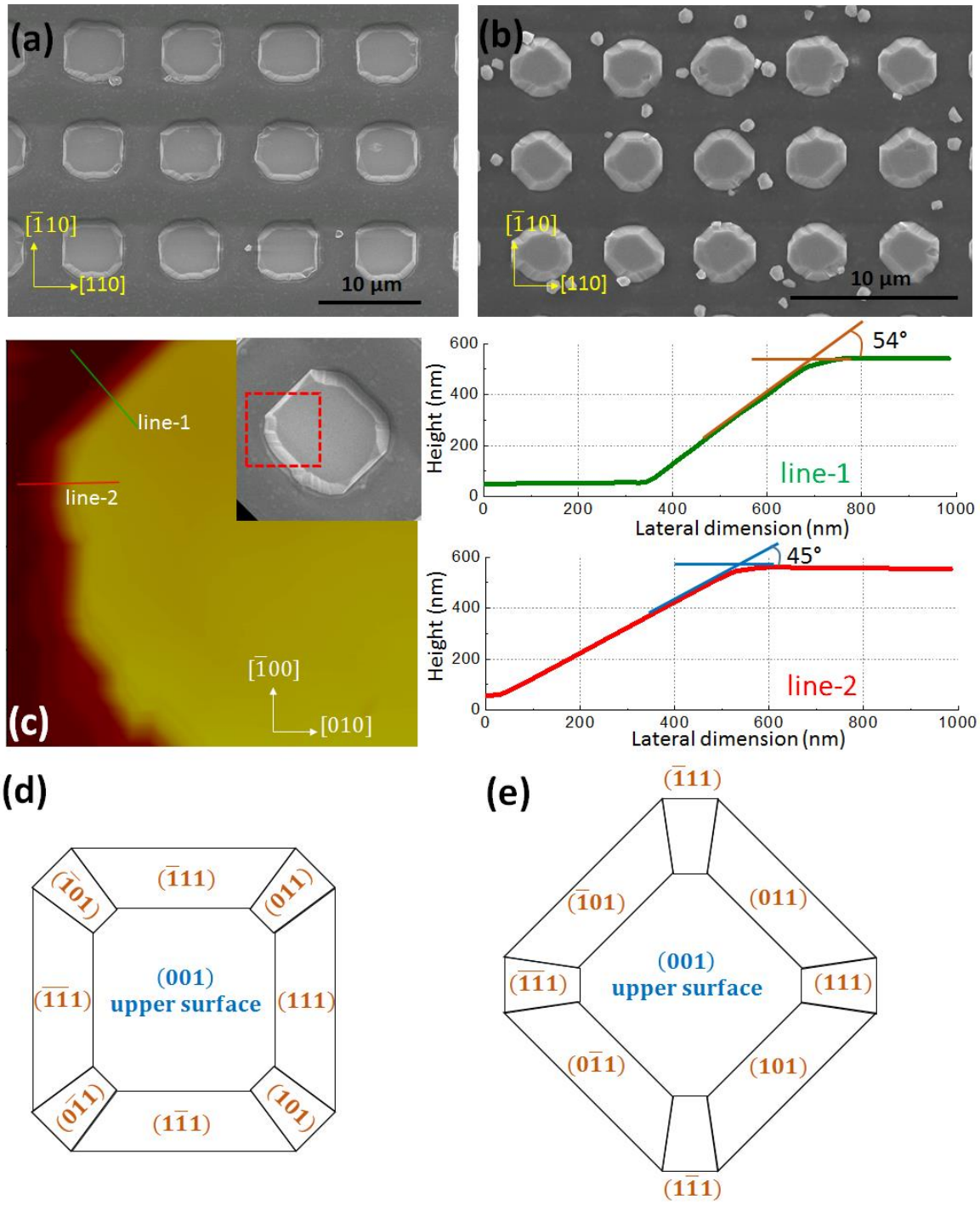

Figure 3. (a)-(b) Top-view SEM images of 5 μm × 5 μm GaAs crystals and 3 μm × 3 μm GaAs crystals; (c)AFM line scan on a 5 μm × 5 μm GaAs crystal showing the sidewall angles with respect to the upper (001) surface; (d)-(e) Sketch of crystallography of epitaxial GaAs disks grown in squares with <110> orientated sides and <100> orientated sides.

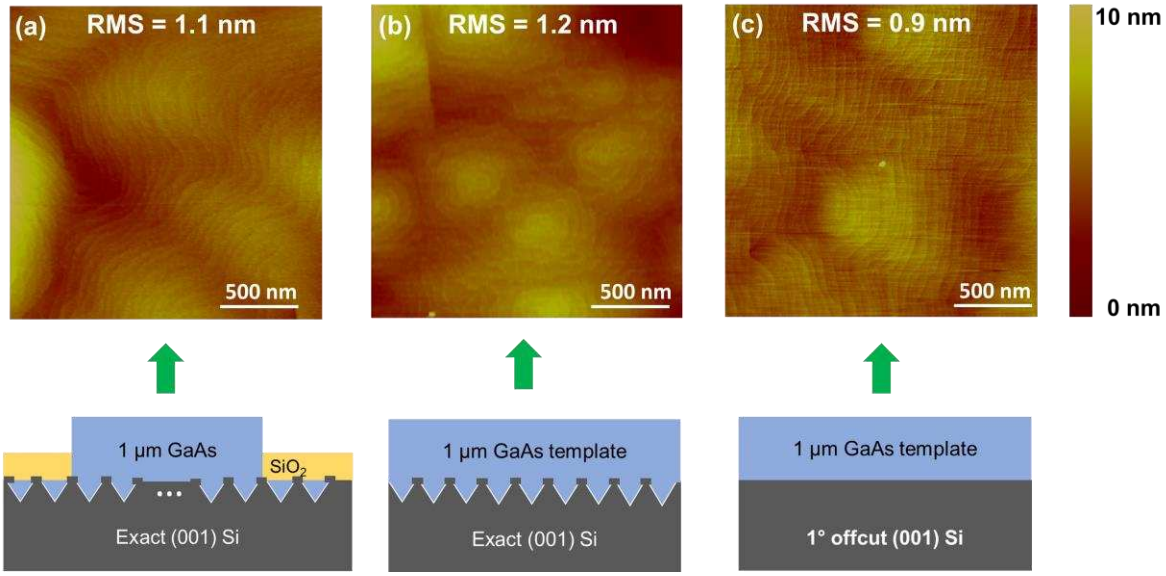

Figure 4. AFM images of the top-surface of GaAs crystals (a), GaAs thin film on V-grooved Si (b), and GaAs thin films grown on planar offcut Si (c).

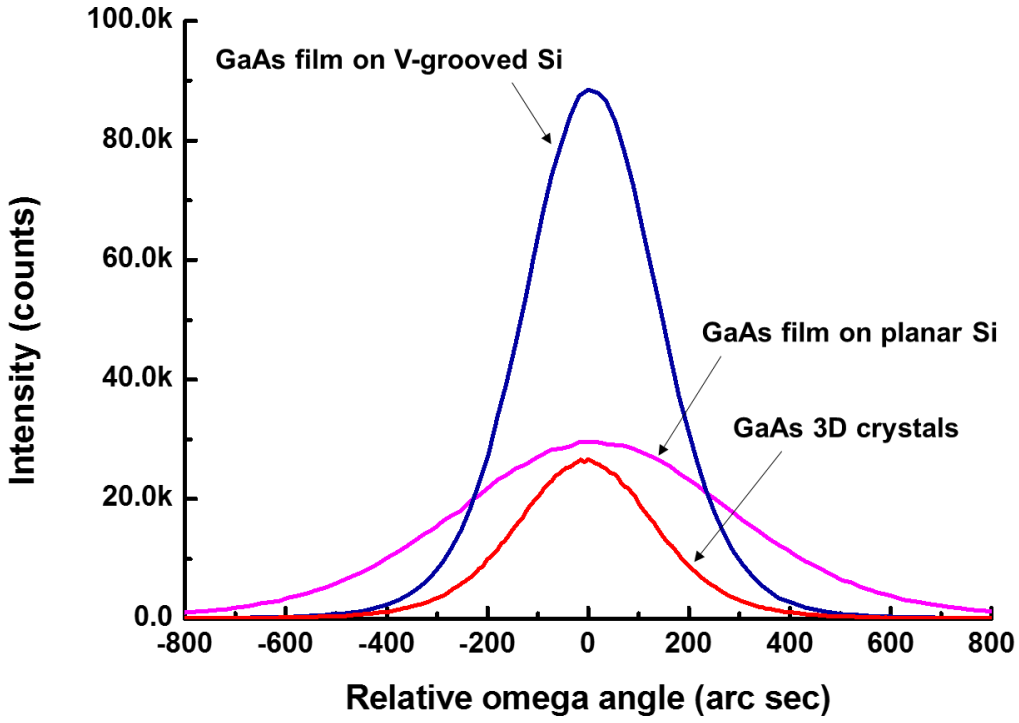

Figure 5. Comparison of XRD omega rocking curves.

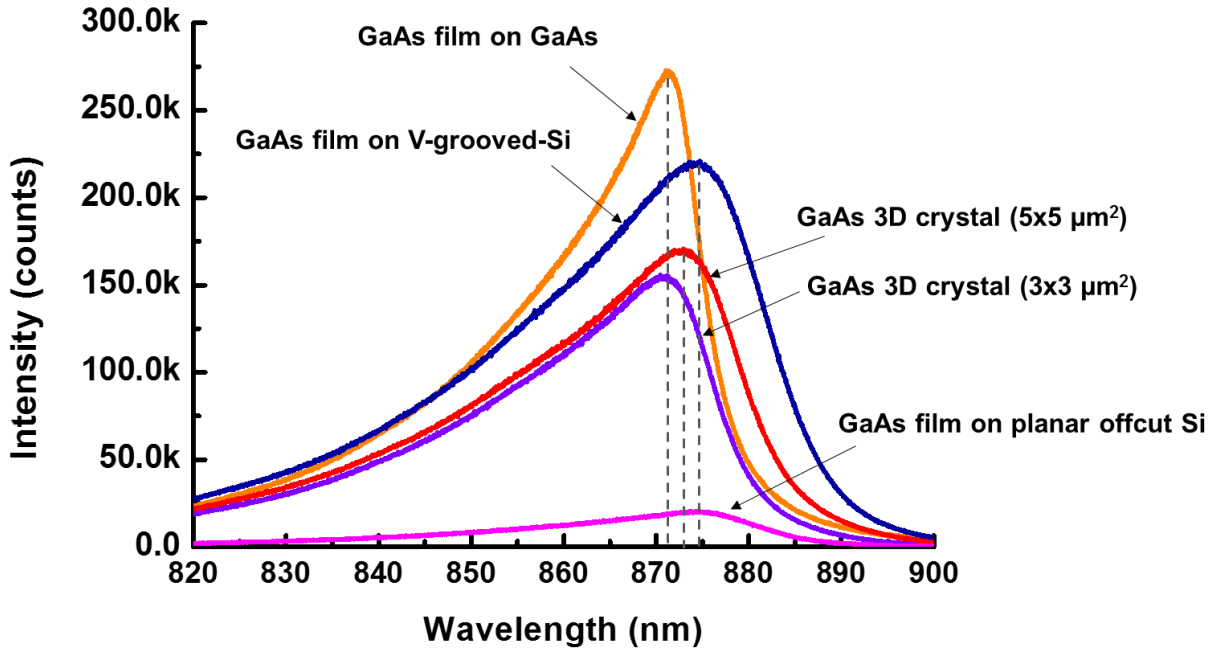

Figure 6. Comparison of room temperate μPL curves of GaAs on Si against the homoepitaxial GaAs reference.